# Suspension Characteristics of Borate-Crosslinked Gels: Rheology and Atomic Force Microscopy Measurements

NAVAL GOEL,[1] SUBHASH N. SHAH,[1] WEI-LI YUAN,[2] EDGAR A. O'REAR[2]

[1] School of Petroleum and Geological Engineering, The University of Oklahoma, Norman, Oklahoma 73069

[2] School of Chemical Engineering and Material Science, The University of Oklahoma, Norman, Oklahoma 73069

*Received 28 December 2000; accepted 16 March 2001*

**ABSTRACT:** Borate-crosslinked guar gels were prepared and characterized to understand their capability to suspend and transport sand particles through a fracture created in a petroleum reservoir. In this study the crosslinked gels were formulated by varying the borate crosslinker concentrations that were selected such that the gels satisfied the minimum viscosity criteria (100 cP at 100/s) used to evaluate crosslinked gels for their suspension capabilities. However, some of these gels did not exhibit satisfactory particles transport through a slot that models a parallel fracture. These gels were then characterized using oscillatory measurements and atomic force microscopy (AFM) to understand the influence of the microscopic behavior of the crosslinked gels on their macroscopic performance in the slot. The results showed that the suspension transport characteristics of these gels could be described through crosslinked networks formed across the guar polymer. The AFM images and rheological measurements of these gels suggest that the elastic modulus provides more useful information than the viscosity about the crosslinked gel structure and their capability to suspend sand particles. © 2001 John Wiley & Sons, Inc. J Appl Polym Sci 82: 2978–2990, 2001

**Key words:** crosslinked gels; atomic force microscopy; rheology; viscoelastic properties; suspensions; fracturing; settling; reservoir stimulation; solids transport

## INTRODUCTION

Suspensions are solids suspended in liquids. Some examples of suspensions are particles in salad dressings, concrete in construction activities, coal in hydraulic transport through pipes, sewage discharged in effluent streams, cement slurries, drilling mud, and sand slurries used in hydraulic fracturing of subterranean formations.[1–4] Each example requires that the solid particles remain suspended in the liquid; otherwise the particles would settle down, plugging lines and creating undesirable solid handling problems. The solids can remain suspended in the liquids with the help of turbulence when the suspensions are transported at high flow rates. However, at low flow rates the suspension properties depend on the carrier liquid capabilities and thus require an understanding of the fluid characteristics.

In hydraulic fracturing a fluid is used to create a fracture in a reservoir and then to transport sand particles through the fractured formation. The sand particles, when placed and uniformly distributed in the fracture, keep it open after the fracturing treatment, allowing oil and gas to eas-

*Correspondence to:* N. Goel (naval@ou.edu).

Contract grant sponsor: U.S. Dept. of Energy; contract grant number: DE-FC21-92 MC29077.

Contract grant sponsor: University of Oklahoma.

Journal of Applied Polymer Science, Vol. 82, 2978–2990 (2001)

ily flow to the surface. The uniform distribution of the solids is achieved with a fluid, which keeps them suspended during the fracturing. Because of the importance of keeping the solids in suspension, an accurate design of the carrier fluid is critical for the success of a fracturing treatment.[5]

Since their introduction in the 1950s, fracturing fluids have been continuously improved from simple oils to sophisticated water-based polymer gels,[6] and numerous patent applications have been filed that describe the unique chemistry used to prepare these fluids. These fluids have been subsequently used around the world.[7–9] Although several fluid formulations have been developed over the years, the method to evaluate the fluid for its capability to suspend and transport solids has remained unchanged.[10–13]

Currently, viscosity is used as a parameter to evaluate fluid for its sand suspension characteristics. An established criterion for a fluid's capability to transport solids is that the fluid should have a minimum viscosity of 100 cP at a shear rate of 100/s over a 3-h test performed at a desired temperature.[10–13] This viscosity is measured using a standard procedure recommended by the American Petroleum Institute (API) to evaluate fracturing fluids.[14] Guar solutions crosslinked with borate ions are the most widely used fluid systems available today. These gels exhibit viscoelastic fluid characteristics. In viscoelastic fluids the viscosity provides a poor description of particle suspension under static fluid conditions.[15] Therefore, under fluid flow conditions, the viscosity would also poorly describe their solids transport characteristics. Thus, there is a need to identify a characteristic property that can be used for evaluating these fluids for their suspension capabilities. This need requires a fundamental understanding of the relationship between the microscopic structure of crosslinked guar gels and their solids transport behavior. This understanding would help to describe the discrepancy in using viscosity to evaluate and identify a fluid property other than the viscosity that would describe the fluid performance for suspension applications.

Thus, in the present study borate-crosslinked guar gels were formulated by varying the crosslinker concentration while keeping all other fluid parameters constant. The gels were evaluated for their solids transport behavior in a slot that models a vertical parallel fracture by preparing slurries at a 20 wt % sand concentration. Then all gels were rheologically characterized using oscillatory measurements and imaged using atomic force microscopy (AFM) to understand the influence of the microscopic structure of the crosslinked gels on their macroscopic performance in the slot.

One unique aspect of this study is the use of AFM imaging to understand the microscopic structures that are formed in the crosslinked gel. Several imaging techniques were previously used to understand polymer gel structures[16–20] but rarely to better understand those of the crosslinked guar gels[21,22] and never to understand the suspension characteristics of a borate-crosslinked guar gel. Thus, by including AFM characterization, this study uses a fundamental approach to correlate fluid behavior with its suspension characteristics. This approach would also help to further understand the borate-crosslinked gels that are widely studied for numerous applications.[23–27]

## EXPERIMENTAL

### Sample Preparation

The fluid formulation consisted of preparing a guar polymer solution at 4.2 g of guar (batch 716001, Economy Polymer, Houston, TX) per 1 L of Norman city water to which a bactericide solution was added to prevent degradation of the guar polymer. The guar concentration ($2.26 \times 10^6$ kg/kg mol molecular weight) was selected to be higher than the overlap concentration of the polymer (1.5 g/L). The solution was allowed to hydrate for 1 h, after which its pH was adjusted to 11. The guar solution was then crosslinked with different quantities of a borate crosslinker solution, which was prepared by mixing 120 g of disodium octaborate tetrahydrate (US Borax, Valencia, CA) in 1 L of water. The crosslinker solution was added at 0.0, 0.25, 0.45, 1.0, and 3.0 mL/L of guar solution to prepare five crosslinked gel samples. These samples were then characterized at ambient temperature for their rheology and AFM imaging.

For the rheological characterization and AFM imaging, the borate solution was injected into 1 L of the guar solution while it was mixed and sheared in a blender. The guar gel thus prepared was further sheared for an additional 3 min to shear precondition it prior to its characterization.[14] The sample was then immediately loaded onto a viscometer for API recommended viscosity tests or a rheometer for oscillatory measurements. For the AFM measurements the gel sample was further sheared for few more seconds

beyond the shear-conditioning period. Then a freshly cleaved natural muscovite mica (V-4 grade, Asheville–Schoonmaker Mica, Newport News, VA) was dipped into the gel to transfer the sample onto the mica surface. The mica was then cleaned around the edges to remove any excess gel, transferred to a closed chamber containing a desiccant, and left to dry. All crosslinked gel samples were prepared at the same time and dried in the closed chamber for 2 days before making the AFM measurements.

The crosslinked gels were directly used in the AFM characterization and were neither diluted nor imaged under alcohol as done earlier to image polysaccharides.[19,28] The present approach was taken because the earlier studies used non-crosslinked gels whose structures were probably not influenced by the presence of water and alcohol. In this study a borate-crosslinked gel was used, and it can be affected by dilution through changes in the gel pH. Because the fluid pH strongly influences the crosslinking chemistry of a borate-crosslinked gel, any change in pH would affect the gel structure and alter its characteristics. Therefore, the gel samples were not interacted with any other chemicals after formulating them in the blender.

### AFM Measurements

The AFM images were acquired with a NanoScope III MultiMode Scanning Probe Microscope (Digital Instruments, Santa Barbara, CA), which is capable of mapping a sample surface in 3 dimensions.[29] The instrument was operated in contact mode and tapping mode. Both these modes were successfully used in earlier studies to image polysaccharide samples.[19,21,30,31] Only the images obtained with the contact mode are shown in this study. The samples were imaged with a sharpened triangular silicon nitride probe with force constants in the range of 0.01–0.6 N/m and a nominal tip radius between 5 and 40 nm.

The crosslinked gels were first imaged with an optical microscope (900-$\mu$m scale) to observe the global features of the sample. Then they were imaged with the scanning probe microscope to capture detailed surface features not visible under the optical microscope.

### API Viscosity Tests

The viscosity tests were performed on a Nordman Viscometer (model 5051, Nordman Instruments, Houston, TX) using a Couette (bob and cup) geometry. The bob had a radius of 15.99 mm and was 87.388 mm in length; the cup, which was also the rotor, had a radius of 18.45 mm and was 136.5 mm long.

The API viscosity test was performed for 3 h at a shear rate of 100/s. During the single shear rate test, a shear rate ramp of 100, 75, 50, 25, 50, 75, and 100/s was performed for a short duration every 30 min.[14] The shear rate ramp was used by the instrument to report test results as power law parameters, the flow behavior index ($n$), and the consistency index ($k$); from these the gel viscosity at 100/s was calculated as a function of time.[14,32] These calculated values are presented in this article.

### Oscillatory Measurements

The viscoelastic measurements were made on a Bohlin rheometer (model CS50, Bohlin Instrument, East Brunswick, NJ) using a cone and plate geometry with a cone angle of 4° and diameter of 40 mm. These measurements were made at a shear strain of 0.05, which was in the linear viscoelastic regime of the fluid.

### Solids Transport and Suspension Tests

The solids transport tests were performed using the large-scale test setup shown in Figure 1. In these tests the guar solution was prepared in fluid mixing tanks, and its pH was adjusted to 11. Then sand (20/40 mesh, Brady Sand) was added to prepare a slurry containing 20 wt % solids. The slurry was then crosslinked by injecting the crosslinker solution with an ISCO syringe pump into an eye of the centrifugal pump. The crosslinked slurry was pumped at 151 L/min through 3000 ft of coiled tubing (1.188-in. i.d.) to simulate a shear-preconditioning rate of 1000/s. This shear conditioning was necessary so that the fluid was subjected to conditions similar to those it faces while flowing during a fracturing treatment.[14] After shearing the crosslinked slurry through the coiled tubing, the slurry was diverted at 38 L/min through a transparent slot model and the balance was pumped off to a disposal tank. The low slurry flow rate through the slot model allowed simulation of a low shear environment (185/s) of a fracture. After being pumped through the slot, the gel was disposed of in a sump tank.

The transparent slot was made of plexiglas, which permitted visual observation of the sand

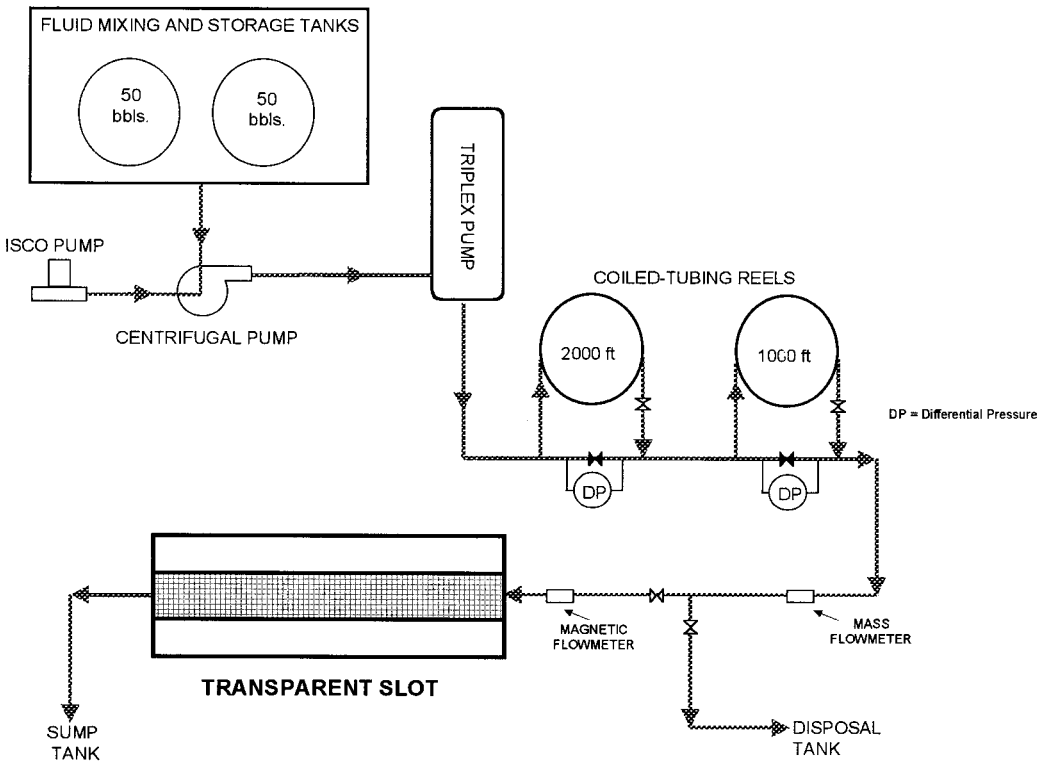


**Figure 1** The schematic of a large-scale experimental setup for solids transport tests.

suspension behavior. The slot was 12 ft long, 20 in. high, and 0.25 in. wide and had a 0.5-in. opening in the inlet to simulate a perforation through which fluid flows into a fracture. The solids distribution in the slot was photographed with a video camera (Panasonic AG-195 P), and the images were stored on a videocassette. A few frames of these video images were digitized and are included in the article to describe the solid transport behavior of the crosslinked gels through the slot.

## RESULTS AND DISCUSSION

### API Viscosity Tests

Figure 2 shows the apparent viscosity at a shear rate of 100/s for the five crosslinked gel samples. The figure shows the viscosity values as averages of the values obtained from the separate test runs. It also shows error bars, which are drawn to describe the range of viscosities measured for various runs.

Figure 2 shows that the guar gel prepared without crosslinker solution had an initial viscosity of 77 cP and a value of 60 cP at the end of the 3-h test. Thus, the guar solution had a lower viscosity than 100 cP. Its viscosity increased beyond 100 cP when the crosslinker solution was added to it. At 0.25 g/L crosslinker concentration the initial viscosity of the crosslinked gel was close to 200 cP, which was reduced to 135 cP after 3 h because of the shear degradation of the gel. Similarly, at 0.45 mL/L the initial viscosity was 260 cP, which stabilized after 3 h to 150 cP, which is close to that of the 0.25 mL/L gel. This trend toward an increase in the gel viscosity with the crosslinker concentration was continued when the crosslinker concentration was increased to 1 mL/L. At this concentration it can be seen that the gel had higher initial and 3-h viscosities than those of the previous three gels. However, the viscosity of the 1 mL/L gel did not stabilize in 3 h as it did in the other two gels. This could be because of a labile nature of the crosslinking bonds in these gels. The crosslinked bonds between the monoborate ions in the crosslinker solution and *cis*-hydroxyl groups on the guar polymer break and reform continuously with the applied shear.[33–35] Also, the lifetime of their interaction is only 1 ms.[35] Thus, the structure and viscosity of the crosslinked guar gels change with

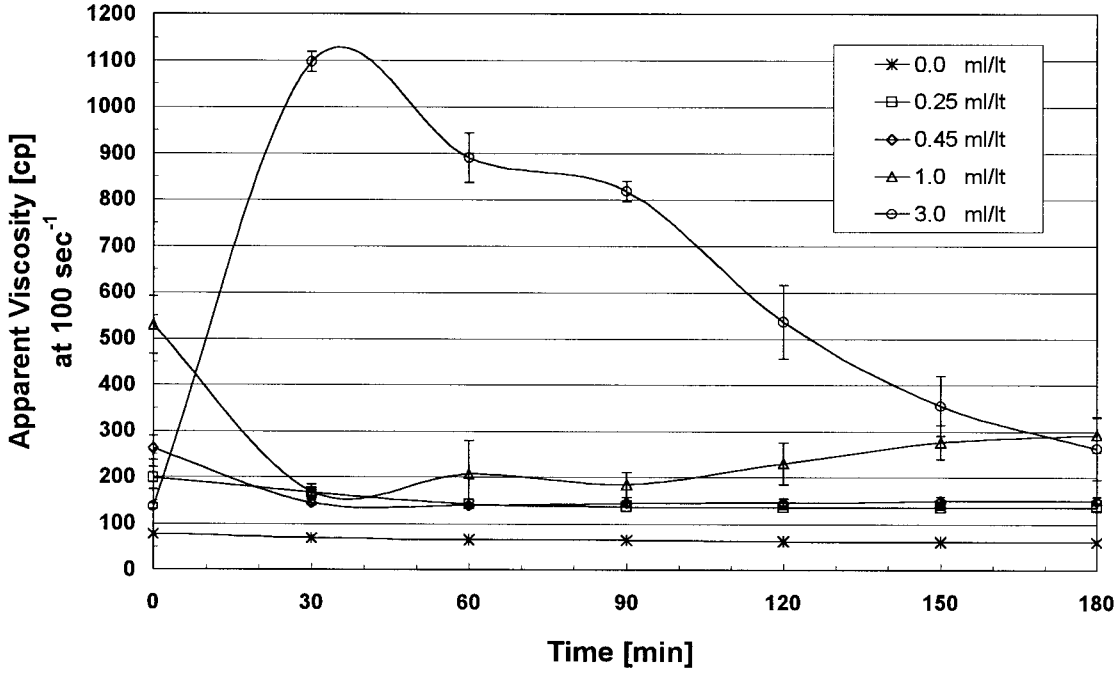


**Figure 2** The API viscosity values of borate-crosslinked guar as a function of the crosslinker concentration (4.2 g/L guar, pH 11, 25°C).

both the shear rate and time. An equilibrium was established between the crosslink bond breaking and reforming during the 3-h evaluation of the 0.25 and 0.45 mL/L gels but not the 1 mL/L gel. The observed behavior is shown in Figure 2.

A similar change was observed in the viscosity of the gel prepared at 3 mL/L, except that this gel had a low initial viscosity. The low viscosity could be because of a very high crosslinker concentration that overcrosslinked this gel. When this gel was sheared in the high shear environment of the blender, it broke down into small gel domains that had poor gel strength and low initial viscosity; but when transferred to the low shear conditions of the viscometer, these domains realigned[21] and crosslinked back together, thereby increasing the gel viscosity. As the gel was sheared further in the viscometer it began to shear degrade; as a result, its viscosity began to decrease with time. In addition to decreasing the fluid viscosity, the high crosslinker concentration in this gel caused it to phase separate. When the gel was kept unsheared for 24 h, it separated into two phases: a crosslinked polymer mass and a water phase containing almost negligible guar polymer. This phase separation of the gel indicates that a fully crosslinked guar gel was formed at the 3 mL/L crosslinker concentration. A similar phase separation was not observed in any other crosslinked gel prepared in this study, indicating that the other gels were not completely crosslinked.

Yet another observation is worth mentioning here. The borate-crosslinked guar gel exhibits normal stresses, so it climbs the viscometer shaft when sheared in a rotational viscometer. After the API viscosity tests a small gel volume was resting on the top of the bob. Because a fixed quantity of the gel sample was loaded in the viscometer, the gel that climbed up the bob came from the annulus between the bob and the cup. An insufficient volume of gel would have remained in the annulus, which was attributable to gel climbing; as a result, the viscometer measured a lower viscosity. This reduction in the gel viscosity is not easy to identify. Because the value that was measured was less than the actual viscosity of the crosslinked gel, it should not affect the minimum viscosity criterion used for the solids suspension in the fluid.

Figure 2 shows that, except for the noncrosslinked gel, all other gels had viscosities greater than 100 cP during the 3-h test. Because these gels have higher viscosities than the minimum reported for satisfactory solid transport,[7,10–13] they should be able to suspend and transport solids through the slot.

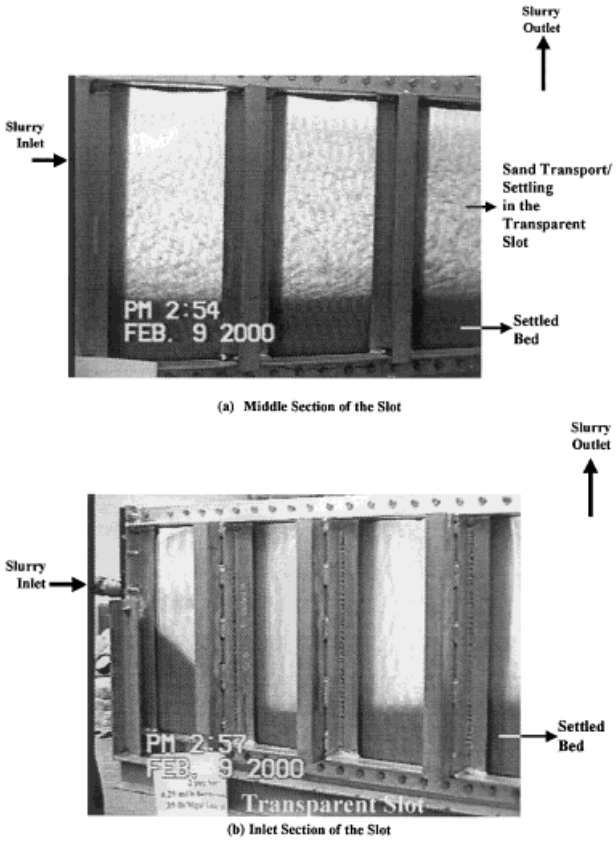


**Figure 3** The sand transport in the transparent slot with 0.25 mL/L borate-crosslinked gel (4.2 g/L guar, pH 11, 25°C, 20 wt % slurry).

### Solids Transport and Suspension Tests

Figure 3 depicts two frames of the video images obtained when a 20 wt % slurry of 0.25 mL/L borate-crosslinked guar gel was pumped through the slot. A settled bed at the slot bottom is evident in the images. The bed formed as soon as the sand slurry was introduced into the slot. The formation of the settled bed implies that the gel was unable to keep particles in suspension and that the solids transport through the slot was inadequate. This undesirable settling displays an unsatisfactory performance for the 0.25 mL/L crosslinked guar gel as a carrier fluid. This behavior occurred despite the gel having higher viscosity than the minimum required for satisfactory solid transport.

The solids transport capability of the crosslinked gel can be improved if the crosslinker concentration is increased. Therefore, another test was performed in which the crosslinker concentration was raised to 0.5 mL/L, which is twice that of the previous test. At the new crosslinker concentration the solids distribution was uniform throughout the slot. Hence, during the test the crosslinker concentration was reduced to 0.45 mL/L and the slurry flow was continued through the slot. At this crosslinker concentration the crosslinked gel was also able to transport sand particles through the slot and no settled bed was formed. This is evident from the sand distribution images shown in Figure 4. Again, because the 0.45 mL/L gel transported sand through the slot, the crosslinker concentration was further reduced to 0.4 mL/L to identify the lowest crosslinker concentration that would carry sand particles through the model. In the 0.4 mL/L crosslinked gel the sand particles began to separate from the gel, displaying that this gel was losing its ability to transport 20 wt % slurry through the slot. The diminishing capability of this gel indicated that 0.45 mL/L was the minimum acceptable crosslinker concentration in this borate-crosslinked guar gel at pH 11 that would satisfactorily transport 20 wt % slurry through the slot.

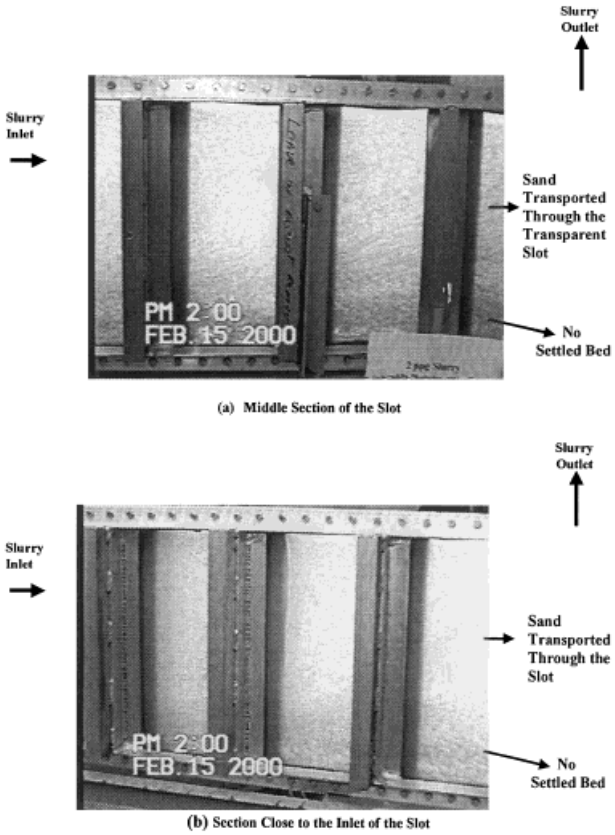


**Figure 4** The sand transport in the transparent slot with 0.45 mL/L borate-crosslinked gel (4.2 g/L guar, pH 11, 25°C, 20 wt % slurry).

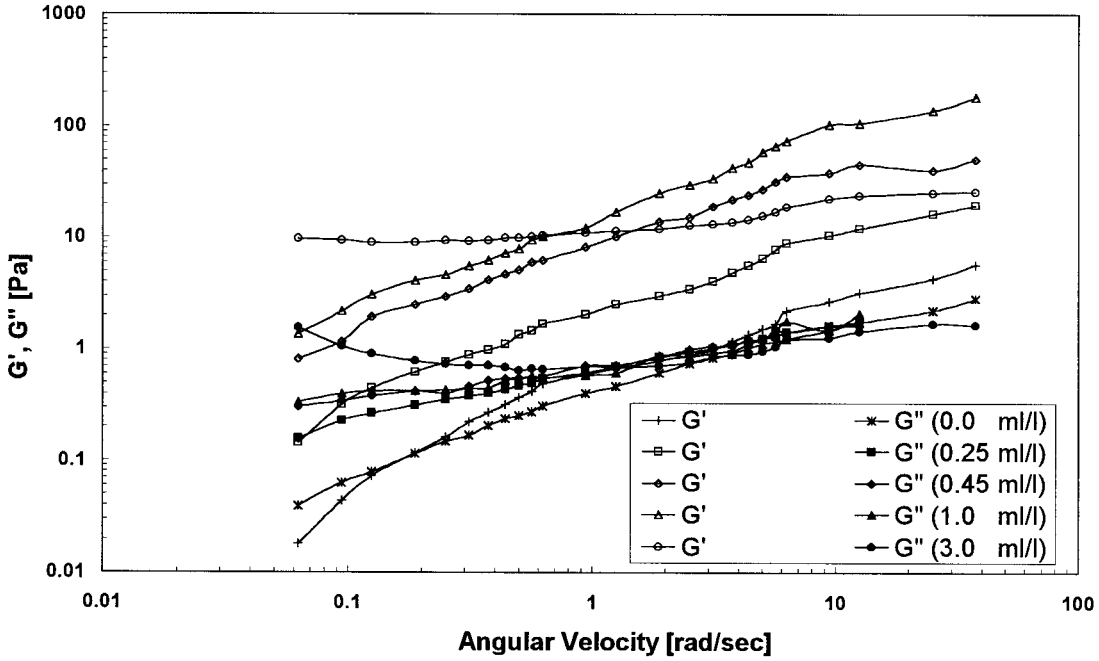


**Figure 5** The oscillatory measurements of borate-crosslinked guar as a function of the crosslinker concentration (4.2 g/L guar, pH 11, 25°C).

Figure 2 shows that the viscosity of the 0.45 mL/L crosslinked gel is higher than 100 cP at 100/s, which was also the case for the gel at 0.25 mL/L. These two gels have similar viscosities but dissimilar suspension capabilities. The 0.45 mL/L gel satisfactorily transported sand particles through the slot whereas the 0.25 mL/L gel did not. Thus, the viscosity could correctly predict the suspension capability of the 0.45 mL/L gel but not that of the 0.25 mL/L gel. Therefore, the viscosity criterion was partially successful in predicting the performance of the carrier fluid. This implies that the present criterion is not completely reliable and is insufficient for characterizing suspension properties of the crosslinked gels.

Because the 0.25 mL/L crosslinked gel could not satisfactorily transport solids through the slot, the gel prepared without crosslinker (i.e., guar polymer solution) would also perform unsatisfactorily as a carrier fluid. On the other hand, because the 0.45 mL/L borate-crosslinked gel described the minimum crosslinker concentration to transport a 20 wt % slurry through the slot model, a gel prepared at 1.0 mL/L would still transport the same slurry. Furthermore, the API viscosity values for the gel prepared at 1.0 mL/L were higher than those of the 0.45 mL/L gel as shown in Figure 2. The gel prepared at 3.0 mL/L concentration sheared into small gel domains and exhibited phase separation, so it would be an unacceptable carrier fluid formulation. As a result, the borate-crosslinked guar gels at 0.0, 1.0, and 3.0 mL/L were not examined for their solids transport behavior in the slot.

The question remains as to why the 0.25 mL/L crosslinked gel exhibited poor suspension characteristics while the 0.45 mL/L gel could satisfactorily transport the 20 wt % slurry through the slot. To understand this, these crosslinked gels were further characterized for their viscoelastic properties and their network structures were imaged using AFM.

## Oscillatory Measurements

Figure 5 shows the elastic and viscous moduli of various borate-crosslinked gels that were investigated. It shows that the elastic and viscous moduli increased as the crosslinker concentration was increased from 0.0 to 3.0 mL/L. The increase in the viscous moduli with the concentration is seen only at low frequencies whereas the increase in the elastic moduli is seen in almost the entire frequency range. This increase in the moduli could be attributed to an increase in the crosslink density of the guar gel. At higher crosslinker concentrations the solutions have more borate ions that could further attach to the *cis*-hydroxyl

groups on the guar polymer to establish more crosslinked bonds between the polymer chains.[33–37] An increase in the number of crosslinked bonds resulted in an increase in the gel moduli at higher crosslinker concentrations.

Figure 5 further shows that, except for the gel prepared at 3 mL/L, the elastic modulus curves of all other gels do not clearly exhibit plateau moduli. The absence of the plateau moduli in the borate-crosslinked gels analyzed here could be explained from a low enthalpy of formation of the crosslink bonds between the borate ions and hydroxyl groups. This low enthalpy means the crosslink bonds can break easily with the energy supplied during the gel shearing. Therefore, when the gel was shear preconditioned in the blender, these bonds broke with the shear and, when the gel was characterized for oscillatory measurements immediately after it, these bonds could not reestablish. As a result, the gels did not exhibit plateau moduli in the rheological measurements performed immediately after shearing in the blender.[38] Because the plateau modulus, which indicates a solidlike characteristic, could be used with rubber elasticity theories to estimate the crosslink density, its absence makes it difficult to quantify crosslinking from the elastic moduli of these gels. Hence, the oscillatory measurements could only suggest that the elasticity and viscosity of the borate-crosslinked gel increased with an increase in the crosslinker concentration. In the 3 mL/L crosslinked gel, however, the crosslinker concentration was so large that, despite the shearing in the blender, a constant elastic modulus ($G'$) is observed at even the lower frequencies. In this gel the $G'$ did not increase at higher frequencies but remained constant at a value similar to that at the lower frequencies. The lower $G'$ of this gel at the higher frequencies as compared to those of the gels prepared at 0.25, 0.45, or 1 mL/L indicates the presence of wall slippage behavior during the oscillatory measurements.[33]

Figure 5 also shows that the borate-crosslinked gels have higher $G'$ than $G''$ values in the entire frequency range in which the gels were evaluated. The higher elastic than viscous modulus means the formation of a polymer chain network in the borate-crosslinked guar gels.[39] However, this well-structured polymer network would not have formed in the 0.25 mL/L gel because it was unable to suspend sand particles in the slot. The network structure might have existed in the 0.45 mL/L and higher concentration gels because of the satisfactory solid transport behavior in the slot. Thus, by merely observing a higher elastic modulus than the viscous modulus, it is difficult to suggest that a network structure exists in borate-crosslinked gels and that the gel would exhibit satisfactory suspension characteristics. Because of these limitations in identifying the gel structure with the rheological measurements, these gels were further characterized using the AFM measurements.

## AFM Characterization

For the AFM measurements the borate-crosslinked gels were transferred to the mica surface by dipping the mica substrates into the gel and then were left to air dry. These gels dried to form films on the substrate. The films were then imaged with an optical microscope and a scanning probe microscope. Because the optical microscope could not identify structures in the gel films, an AFM microscope was used to explore microscopic features in the gel.

The AFM images depicted that the gel dried into three distinguishable regions: a thin-film region left behind by the evaporated water and containing a nominal amount of polymer, a polymer-rich region where the guar fibers were distinctly seen in the image, and a thick-film region where the gel dried into grains containing fractals of polymer mass. These three regions are shown in the AFM images of Figure 6 for the 4.2 g/L guar solution.

Figure 6(a) shows the thin-film region with no polymer fiber seen in the image. The figure depicts this film as having a number of tiny pinholes, which are uniformly distributed on the image. Similar pinholes were observed in the AFM images of all gel samples. At some locations on the mica substrate these pinholes were visible with the AFM instrument [Fig. 6(a)], and at others they were covered by guar fibers and hence could only be seen under the fibers in the AFM images of the crosslinked gels. The presence of pinholes in all samples indicates that the thin film could be covering the entire mica surface. This thin film might have formed from the water used to prepare the guar solution. Because this water contained some chemicals added for uniform dispersion of guar in the solution, it dried to leave a thin film. Thus, this film might contain some guar polymer and chemicals that might be deposited due to different affinities of the guar polymer and the solvent to the mica substrate. Furthermore, this film could be formed because of

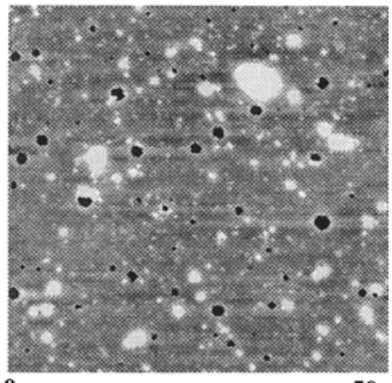


(a) Thin-Film

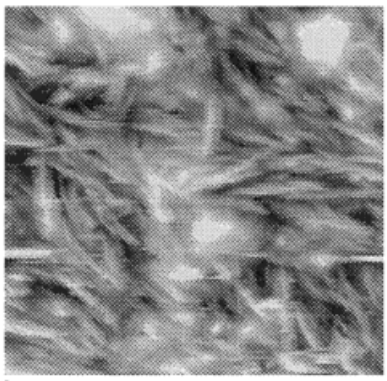


(b) Polymer-Rich Region

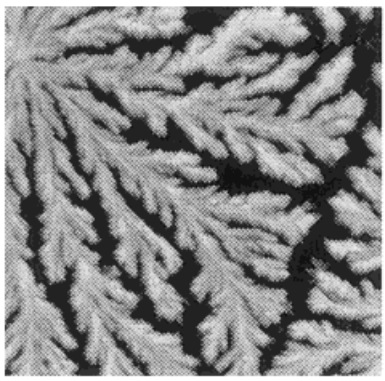


(c) Thick-Film

**Figure 6** AFM images of the 4.2 g/L guar solution at pH 11 and 25°C.

an incomplete molecular dispersion of guar polymer in the solution, because that has been seen in water soluble polymers.[40] The significance of this film is not well understood at this point.

Figure 6(b) shows the polymer-rich region where the polymer fibers are seen as randomly oriented small, short fibrils. These fibrils overlap, indicating that the guar concentration in the prepared solution is higher than its overlap concentration. The fibrils seemed to have a strong interaction with the AFM probe, resulting in undesirable noisy lines in the image.

Figure 6(c) shows the thick-film region where the guar fibers are not individually visible but are seen as a large polymer grain of the fractal structures. The grain had a nucleus from which leafy branches were radially spreading. The thick-film region contained several similar grains, and each grain had a nucleus and leaves and was separated from other grains at a boundary. This boundary seemed to result from depletion of guar and not from cracking of the guar film on drying because the leafy branches in the neighboring grains were oriented in opposite directions. The fractals were about 3 $\mu$m in thickness and had a wide range of sizes and densities. The number density of these fractal grains decreased in the gels as the crosslinker concentration was increased. The decrease in their densities indicates that the number of grains increased so much in the gel that the boundaries between them were not clearly demarcated, and so the leafy structures became unidentifiable. Thus, the diminishing fractal pattern in the thick-film region indicates differing structures in the gels prepared at different crosslinker concentrations. As compared to the thick-film region, the polymer-rich region provided more distinguishable features on the crosslinked gel samples. Therefore, the polymer-rich regions were identified on these samples and these were then used to understand the relationship of the network structures formed in the gels to their sand transport characteristics.

Figure 7 shows AFM images in the polymer-rich region of the gels prepared at different crosslinker concentrations. Figure 7(a) shows the image of the gel prepared at a 0.25 mL/L crosslinker concentration. It shows that the addition of the crosslinking agent maintained the fibrous structure in the guar. Because the size of the fibers in this image is larger than that of the guar solution, the fibers would have come from the aggregation of fibrils. The crosslinking agent joined the guar together into a network of polymeric fibers. Underneath this network of fibers the thin-film region containing pinholes can be seen at the bottom right corner of the image. The AFM image further shows that the crosslinker concentration in this gel was not at a high concentration because the fibers were not completely joined together and some of them had dangling ends that

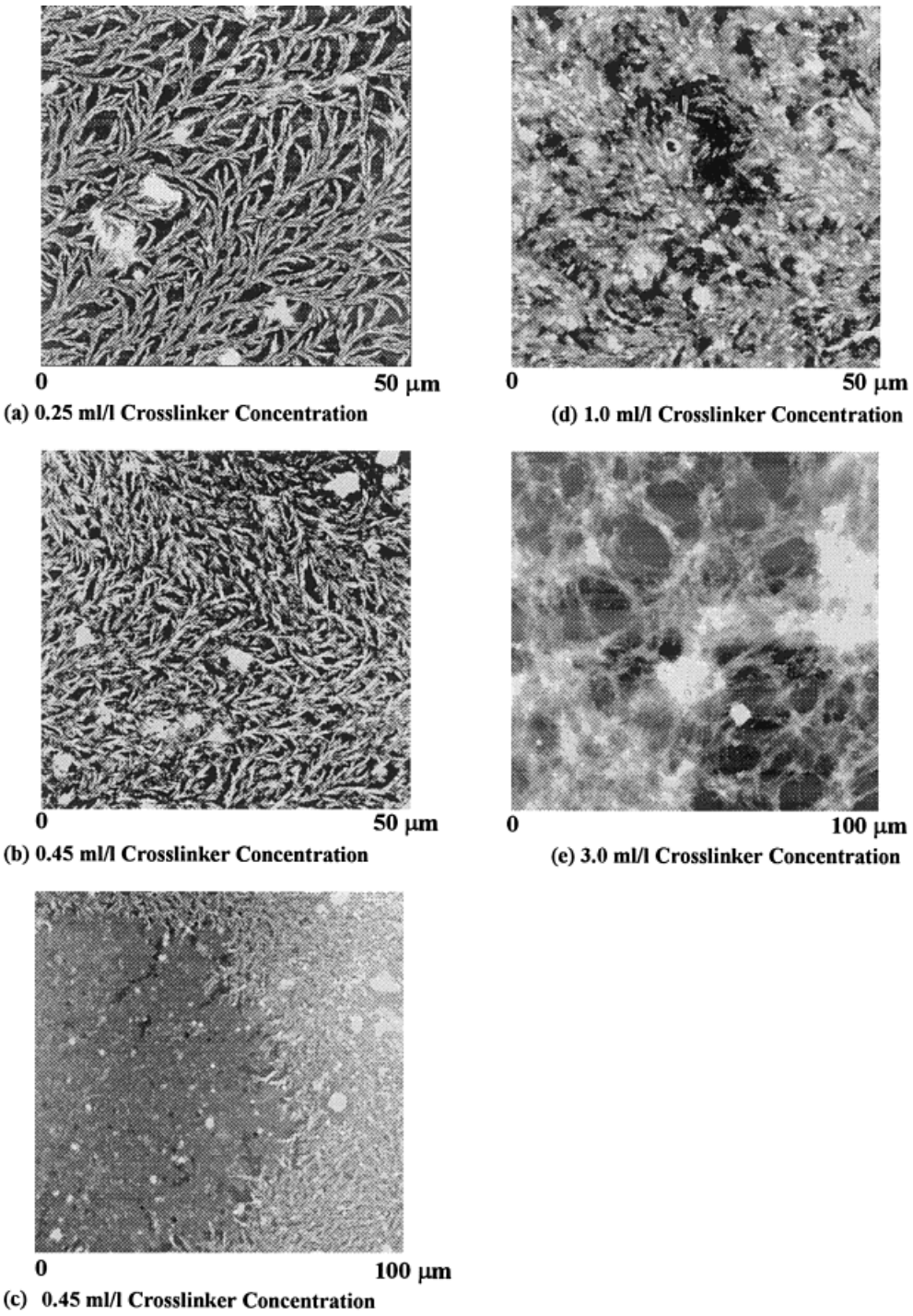


**Figure 7** AFM images of borate-crosslinked guar as a function of the crosslinker concentration (4.2 g/L guar, pH 11, 25°C).

were not crosslinked to any other fiber. The image also shows void spaces between the fibers, indicating a low crosslink density in the sample. Because of the low fiber density, the AFM image suggests that this gel might not have sufficient strength to sustain the weight of the sand particles. Therefore, this gel would not suspend solids through a slot.

When the crosslinker concentration was increased to 0.45 mL/L, more fibers combined together, as seen in the AFM image of the gel in Figure 7(b). The fiber density increased in this gel, leaving very little void between the fibers and little exposure of the lower layer under the fibers. The higher fiber density strengthened the gel and improved its ability to suspend solids through the slot, as seen in the sand transport behavior of this gel.

Figure 7(b) further shows that the guar fibers, although more crosslinked than the 0.25 mL/L gel, are still distinguishable as fibers in the image. Therefore, the fibers were still in a 2-dimensional network structure in the 0.45 mL/L gel. This implies that the gel prepared at 0.45 mL/L might have enough strength to transport a 20 wt % slurry, but it could be unable to suspend solids at higher sand concentrations. Because fracturing fluids are used to transport solids at concentrations up to 60 wt %, another gel with a crosslinker concentration higher than 0.45 mL/L would be required to suspend and transport higher concentration solids through the slot.

Unlike the AFM image for the 0.25 mL/L gel, where the thin-film layer was visible under the fiber, Figure 7(b) does not reveal this film. However, the thin film can be seen near the rim of the polymer fibers shown in Figure 7(c), where this film is visible to the left of the fiber-rich region. This image displays a unique separation between the thin film and the fibers and demonstrates the location of the polymer-rich region on the borate-crosslinked guar gels.

To exhibit changes in the gel structures at higher crosslinker concentrations, a gel was prepared at a crosslinker concentration of 1 mL/L, which is about twice the minimum concentration (0.45 mL/L) required to transport 20 wt % slurry through the slot model. The AFM image of this borate-crosslinked gel is shown in Figure 7(d). It shows that the individual fibers could not be recognized here as they were in the image for the 0.45 mL/L gel. At 1 mL/L concentration the guar gel structure had wide and long fibers. The fibers seemed to be connected with one another to form a thicker multilayered structure, which was uniformly distributed throughout the image. This AFM image suggests that the gel prepared at 1 mL/L would have better strength than the gel prepared at the lower crosslinker concentrations. As the crosslinker concentration was further increased, the gel continued to evolve into a 3-dimensional network, as seen in the AFM image of the 3 mL/L gel in Figure 7(e). At this crosslinker concentration the image shows the crosslinked gel to be concentrated into small polymer-rich regions that are interspersed with water phase regions. This image also shows the fiber aggregates as being connected together by threads of fibers, giving a tissuelike structure to the gel.

While taking the AFM images, the crosslinked gels prepared in the blender were set aside in beakers to observe any distinguishable features in these gels. After 2 days a mica disk was dipped into these gel samples, and interesting observations were made. In the gels prepared at the lower crosslinker concentrations of 0.25 and 0.45 mL/L, the mica disk could be easily inserted in the gel and pulled out with the gel intact in the beaker, showing good mobility of the guar fibers in these gels. On the other hand, in the gel prepared at 1 mL/L, when the mica disk was pulled out of the gel, it lifted the gel along with it as if the gel were a single unit of polymer mass. The gel was lifted to a substantial height before it bounced back into the beaker. This behavior indicates that the guar fibers were well connected with one another and might have formed a 3-dimensional structure at this crosslinker concentration. However, in 3 mL/L gel a very different behavior was observed. At this concentration the gel exhibited phase separation with a solid gel mass floating over a polymer-free solution. This solution was checked for its viscosity and found to have a viscosity similar to that of water. The absence of guar in the phase separated water indicates that the entire guar was concentrated into the gel mass. Furthermore, when the mica disk was inserted into this gel mass, the mica could cut through the gel. Even when the mica was pulled out, the gel neither pulled up with the mica nor rehealed the cut, suggesting that an immobile gel network formed in the 3 mL/L gel. This immobility indicates diminishing viscous characteristics of the gel. These observations imply that the borate-crosslinked gel changed from a viscous fluid to a viscoelastic material and finally to a solid gel when the crosslinker concentration was increased from 0.25 to 3 mL/L.

Because the AFM measurements were made on the dried gel samples, the images do not correctly show the actual structure formed in the gel whose suspension characteristics were evaluated in the slot. However, the AFM images do describe the gels' behavior, which helps to understand

their suspension capabilities. The images suggest the polymer fibrils overlapped in the guar solution. As the crosslinking agent was added to the guar solution, the fibrils crosslinked together into fibers. These fibers aggregated and integrated into a strong network as the crosslinker concentration was increased. At even higher crosslinker concentration the fibers merged together to form wider leaves, making it difficult to identify individual fibers in the image. The fibrous structure continued to develop in the crosslinked gel till the polymer fibers were concentrated into a gel mass, leaving water as a separate phase.

### Fluid Property for Its Suspension Capability

Because the viscosity is viewed as insufficient to describe the solids transport behavior of a borate-crosslinked gel, a question may be raised regarding a better way to characterize carrier fluids in the laboratory.

The AFM images of Figure 7 show that the increase in crosslinking results in an increase in the fiber density and hence an increase in the gel strength. Similarly, Figure 5 shows an increase in the elastic and viscous moduli of the gels with an increase in the crosslinker concentration. These changes in the gel rheology with the crosslinker concentration correspond well with the AFM images of the gel. Figure 5 further shows that the increase in the viscous moduli is less distinct than the increase in the elastic moduli when the crosslinker concentrations were increased from 0.25 to 3.0 mL/L. Figure 2 shows a very small difference in the viscosity of the gels prepared at 0.25 and 0.45 mL/L, even though these gels had a very large difference in the sand suspension characteristics as evidenced in Figures 3 and 4. Thus, the difference in the solids transport characteristics is better described by the large difference in the elastic moduli than in the viscous moduli of these two gels. Therefore, the borate-crosslinked gels characterized by their elastic moduli provided useful information about the crosslinked gel structure and their capability to suspend and transport sand particles. Moreover, the elastic modulus is a better property than the viscosity to characterize and evaluate carrier fluids for their suspension characteristics and it should be further evaluated in a carrier fluid to establish a minimum criterion for satisfactorily transporting solids.

## CONCLUSIONS

The viscosity criterion currently used in the industry provides an insufficient method to evaluate crosslinked fluids for their solids transport characteristics. The suspension capability of these gels was observed as being attributable to an increase in the fiber density across the gel. With an increase in the crosslinker concentration, the borate-crosslinked gels exhibited an increase in the density of the gel network as seen in the AFM images and increases in the elastic and viscous moduli as seen from the rheology characterizations. Consequently, the capability of the gel to suspend and transport solid particles through the slot also increased. On comparing the gel characteristics from the AFM images and the rheological measurements, the elastic modulus seems to provide useful information about the suspension capabilities of the borate-crosslinked gels.

The authors wish to thank the U.S. Department of Energy and the University of Oklahoma for their joint sponsorship of this work and permission to prepare this manuscript. We also appreciate help from the WCTC research team without whom this study would not have been completed. Discussions with Phil Harris (Halliburton) and Bob Smith (US Borax) on borate crosslinking and suggestions by Harold Brannon (BJ services) on AFM images are greatly appreciated.

## REFERENCES

1. Zukoski, C. F. Chem Eng Sci 1995, 50, 4073.
2. Nelson, R. D. In Handbook of Powder Technology; Williams, J. C., Allen, T., Eds.; Elsevier: Amsterdam, 1988.
3. Veziroglu, T. N., Ed. Particulate Phenomena and Multiphase Transport; Hemisphere: Washington, DC, 1988; Vol. 4.
4. Schramm, L. L., Ed. Suspensions: Fundamentals and Applications in the Petroleum Industry; ACS Advances in Chemistry Series 251; American Chemical Society: Washington, DC, 1996.
5. Armstrong, K.; Card, R.; Navarrete, R.; Nelson, E.; Nimerick, K.; Samuelson, M.; Collins, J.; Dumont, G.; Priaro, M.; Wasylycia, N.; Slusher, G. Oilfield Rev 1995, Autumn, 34.
6. Jennings, A. R. J Pet Technol 1996, July, 604.
7. Nimerick, K. H.; Temple, H. L.; Card, R. G. Soc Pet Eng J 1997, 2, 150.
8. Powell, R. J.; McCabe, M. A.; Slabaugh, B. F.; Terracina, J. M.; Yaritz, J. G.; Ferrer, D. SPE Prod and Facilities 1999, May, 139.

9. Dawson, J. C.; Le, H. V.; Cramer, D. Paper (SPE 49042) presented at the SPE Annual Technical Conference and Exhibition, New Orleans, September 27–30, 1998.
10. Free, D. L. U.S. Pat. 3,974,077, 1976.
11. Wadhwa, S. K. U.S. Pat. 4,514,309, 1985.
12. Nelson, E. B.; Constien, V. G.; Cawiezel, K. E. U.S. Pat. 5,658,861, 1997.
13. Dawson, J. C.; Hoang, V. L.; Kesavan, S. U.S. Pat. 6,017,855, 2000.
14. API RP 39: API Recommended Practices on Measuring the Viscous Properties of a Cross-Linked Water-Based Fracturing Fluid, 3rd ed.; American Petroleum Institute: Washington, DC, 1998.
15. Van den Brule, B. H. A. A.; Gheissary, G. J Non-Newtonian Fluid Mech 1993, 49, 123.
16. Nitta, T.; Haga, H.; Kawabata, K.; Abe, K.; Sambongi, T. Ultramicroscopy 2000, 82, 223.
17. Hirokawa, Y.; Jinnai, H.; Nishikawa, Y.; Okamoto, T.; Hahimoto, T. Macromolecules 1999, 32, 7093.
18. Donatelli, A. A.; Sperling, L. H.; Thomas, D. A. Macromolecules 1976, 9, 671.
19. Gunning, A. P.; Kirby, A. R.; Ridout, M. J.; Brownsey, G. J.; Morris, V. J. Macromolecules 1996, 29, 6791.
20. Adriaensens, P.; Pollaris, A.; Vanderzande, D.; Gelan, J.; White, J. L.; Kelchtermans, M. Macromolecules 2000, 33, 7116.
21. Power, D.; Larson, I.; Hartley, P.; Dunstan, D.; Boger, B. V. Macromolecules 1998, 31, 8744.
22. Zasadzinski, J. A. N.; Chu, A.; Prud'homme, R. K. Macromolecules 1986, 19, 2960.
23. Wise, E. T.; Weber, S. G. Macromolecules 1995, 28, 8321.
24. Kesavan, S.; Prud'homme, R. K. Macromolecules 1992, 25, 2026.
25. Sato, T.; Tsujii, Y.; Fukuda, T.; Miyamoto, T. Macromolecules 1992, 25, 3890.
26. Shibayama, M.; Takeuchi, T.; Nomura, S. Macromolecules 1994, 27, 5350.
27. Smith, R. A.; McBroom, R. B. In Kirk–Othmer Encyclopedia of Chemical Technology, 4th ed.; Wiley: New York, 1992; Vol. 4, p 365.
28. Kirby, A. R.; Gunning, A. P.; Morris, V. J. Biopolymers 1996, 38, 355.
29. Magonov, S.; Heaton, M. G. Am Lab 1998, 30(10), 9.
30. Vuppu, A. K.; Garcia, A. A.; Vernia, C. Biopolymers 1997, 42, 89.
31. McIntire, T. M.; Tenner, R. M.; Brant, D. A. Macromolecules 1995, 28, 6375.
32. Gdanski, R. D.; Harris, P. C.; Lord, D. L.; Reidenbach, B.; Shah, S. N. Paper (SPE 21647) presented at the 1991 SPE Production Operations Symposium, Oklahoma City, OK, April 7–9, 1991.
33. Schultz, R. K.; Myers, R. R. Macromolecules 1969, 2, 281.
34. Sinton, S. W. Macromolecules 1987, 20, 2430.
35. Kramer, J.; Prud'homme, R. K.; Wiltzius, P.; Mirau, P.; Knoll, S. Colloid Polym Sci 1988, 266, 1.
36. Prud'homme, R. K.; Constien, V.; Knoll, S. In Polymers in Aqueous Media; Glass, J. E., Ed.; ACS Advances in Chemistry Series 223; American Chemical Society: Washington, DC, 1989; p 89.
37. Pezron, E.; Ricard, A.; Lafuma, F.; Audebert, R. Macromolecules 1988, 21, 1121.
38. Maerker, J. M.; Sinton, S. W. J Rheol 1986, 30 , 77.
39. Tayal, A.; Pai, B. V.; Khan, S. A. Macromolecules 1999, 32, 5567.
40. Robinson, G.; Ross-Murphy, S. B.; Morris, E. R. Carbohydr Res 1982, 107, 17.